Biomaterials 34 (2013) 5747–5758

Contents lists available at SciVerse ScienceDirect

Biomaterials

journal homepage: www.elsevier.com/locate/biomaterials

The molecular mechanism of mediation of adsorbed serum proteins to endothelial cells adhesion and growth on biomaterials

Dayun Yang [a], Xiaoying Lü [a,*], Ying Hong [b], Tingfei Xi [c], Deyuan Zhang [d]

[a] State Key Laboratory of Bioelectronics, School of Biological Science and Medical Engineering, Southeast University, Nanjing 210096, PR China
[b] Nanjing Drum Tower Hospital, Nanjing 210008, PR China
[c] Shenzhen Research Institute, Peking University, Shenzhen 518055, PR China
[d] R&D Center of Lifetech Scientific (Shenzhen) Co., Ltd, Shenzhen 518057, PR China

ARTICLE INFO

Article history:
Received 6 February 2013
Accepted 13 April 2013
Available online 7 May 2013

Keywords:
Biomaterial surface
Protein adsorption and cell adhesion
Molecular mechanism
Proteomics and bioinformatics
Verification experiment

ABSTRACT

To explore molecular mechanism of mediation of adsorbed proteins to cell adhesion and growth on biomaterials, this study examined endothelial cell adhesion, morphology and viability on bare and titanium nitride (TiN) coated nickel titanium (NiTi) alloys and chitosan film firstly, and then identified the type and amount of serum proteins adsorbed on the three surfaces by proteomic technology. Subsequently, the mediation role of the identified proteins to cell adhesion and growth was investigated with bioinformatics analyses, and further confirmed by a series of cellular and molecular biological experiments. Results showed that the type and amount of adsorbed serum proteins associated with cell adhesion and growth was obviously higher on the alloys than on the chitosan film, and these proteins mediated endothelial cell adhesion and growth on the alloys via four ways. First, proteins such as adiponectin in the adsorbed protein layer bound with cell surface receptors to generate signal transduction, which activated cell surface integrins through increasing intracellular calcium level. Another way, thrombospondin 1 in the adsorbed protein layer promoted TGF-β signaling pathway activation and enhanced integrins expression. The third, RGD sequence containing proteins such as fibronectin 1, vitronectin and thrombospondin 1 in the adsorbed protein layer bound with activated integrins to activate focal adhesion pathway, increased focal adhesion formation and actin cytoskeleton organization and mediated cell adhesion and spreading. In addition, the activated focal adhesion pathway promoted the expression of cell growth related genes and resulted in cell proliferation. The fourth route, coagulation factor II (F2) and fibronectin 1 in the adsorbed protein layer bound with cell surface F2 receptor and integrin, activated regulation of actin cytoskeleton pathway and regulated actin cytoskeleton organization.

1. Introduction

Biomaterial–protein interactions and biomaterial–cell interactions are two important scientific issues in the research of biocompatibility of biomaterials. Actually, protein adsorption is the first biological event occurred on biomaterial surface, followed by cell adhesion and growth, when biomaterials are implanted in vivo or tested in vitro [1]. The types, concentrations and conformations of adsorbed proteins play decisive role in subsequent cell response to the biomaterials [2], which can significantly affect the cell adhesion, spreading, migration and proliferation [3,4]. Herein, to understand the mechanism of cells interact with materials, the internal correlated three aspects, the "material surface-protein adsorption", "material surface-cell behavior" and "protein adsorption-cell behavior", must be systematically studied.

However, most of the researches to date are carried out separately on the three aspects. In the study of "material surface-protein adsorption", a variety of methods including isotope labeling, quartz crystal microbalance, ellipsometry, ultraviolet absorption assay and biosensors were used to study proteins adsorption on biomaterials [5–8]. However, these studies mainly focused on investigation of one or several specific proteins adsorption. In fact, the identified blood proteins are more than one thousand kinds [9]. Hence, when biomaterials implanted in vivo or tested in vitro, a variety of proteins from blood or serum containing culture medium will competitively adsorb on the surface to form a composite protein layer. Proteomics technology, a powerful tool for high-throughput investigates components of protein layer, has been used in study

* Corresponding author. Tel.: +86 25 83793430; fax: +86 25 83792882.
E-mail address: luxy@seu.edu.cn (X. Lü).

0142-9612/$ – see front matter © 2013 Elsevier Ltd. All rights reserved.
http://dx.doi.org/10.1016/j.biomaterials.2013.04.028

of serum and plasma proteins adsorption on biomaterials such as titanium and hydroxyapatite [10,11]. However, the mediation of protein layer components to subsequent cell behavior was not studied.

In the study of "material surface-cell behavior", researchers have examined various cell behaviors such as cell adhesion, morphology and proliferation on different biomaterial surfaces by using a variety of cytological methods [12,13]. However, the mediation of cell behavior by adsorbed proteins has usually been skipped over.

For the "protein adsorption-cell behavior" study, focus is on investigating the mediation of some specific proteins (e.g., fibronectin) adsorption or immobilized polypeptide (such as those containing arginine–glycine–aspartic acid (RGD) sequence) on biomaterials to cell adhesion and migration. The results showed that the adsorbed protein or immobilized polypeptide could distinctly promote cell focal adhesion formation, cell adhesion, spreading and migration [14,15]. However, they did not explain the mechanism of adsorbed protein-mediated cell behavior. In other words, with the results from these studies we can only know whether the adsorbed protein has effect on cell adhesion and growth, but don't know how the adsorbed protein mediates cell behavior at molecular level. In addition, cell behavior on biomaterials is mediated by a variety of proteins in adsorbed protein layer rather than single protein. Therefore, the mechanism of mediation of adsorbed protein layer components to cell behavior can be in-depth understood only on the basis of proteomics analysis of adsorbed protein layer on biomaterial.

NiTi alloy has been widely used in the interventional treatment of cardiovascular disease due to its shape memory and superelasticity. TiN coating was used to reduce nickel release from NiTi alloy for improved biocompatibility [16]. Since chitosan has good biocompatibility and biodegradability, it has been explored in wound healing, drug delivery and tissue engineering application [17]. However, it was reported that pure chitosan film had a certain inhibitory effect on cell adhesion and proliferation [18] and the decrease of cell adhesion was correlated with the reduction of protein adsorption [19,20]. Therefore, study of protein adsorption on the NiTi alloys and chitosan film will contribute to fully understanding of the biocompatibility of these materials. To our knowledge, there is no report on proteomics analysis of serum protein adsorption on these materials. Herein, the aim of this study is to systematic investigate the molecular mechanism of mediation of adsorbed serum protein layer components to endothelial cells adhesion and growth on the three biomaterials (biomaterials–proteins adsorption–cell adhesion and growth) using cytological experiments, proteomic technology and bioinformatics analysis, as well as cellular and molecular biology verification experiments.

2. Materials and methods

2.1. Sample preparation and characterization

The bare and TiN-coated NiTi alloy discs with diameter of 6 and 52 mm and thickness of 1 mm were supplied by Lifetech Scientific (Shenzhen) Co., Ltd, China. TiN coating onto polished NiTi (50.8 at% Ni) alloy disc was prepared using vacuum filtered arc plasma deposition technique, and the coating thickness was about 1 μm. The NiTi alloy samples were cleaned by ultrasonication in acetone, ethanol and ultrapure water for 10 min each before experiment. Chitosan powder (Jinan Haidebei Marine Bioengineering Co., Ltd., China) with a deacetylation degree of 85% was dissolved in 1% (v/v) acetic acid to formulate 2% (w/v) chitosan solution, and then centrifuged for degassing. Chitosan films were spin-coated at a speed of 3000 rpm for 3 min on clean glass with 1 mm thickness. After evaporation in a convection oven at 45 °C for 12 h, the yield chitosan films were soaked into 1% (w/v) NaOH solution for 24 h to neutralize the residual acetic acid, followed by rinsed with ultrapure water to be neutral and finally dried in convection oven at 45 °C. The average thickness of the chitosan films was 477 nm as determined by Dektak3ST surface profile measuring system (Veeco Instruments Inc., USA). Each side of the bare and TiN-coated alloys as well as chitosan films was sterilized for 1 h using a UV lamp before biological experiments.

The surface morphology of the bare NiTi alloy, TiN-coated NiTi alloy and chitosan film was examined by Nanoscope IIIa atomic force microscopy (AFM, Digital Instrument Corp., USA). Imaging was performed in tapping mode with a silicon tip. All samples were analyzed in air at room temperature. The root mean square (Rms) roughness was determined under a scan range of $1.5 \times 1.5\ \mu m^2$, using NanoScope software version 4.32r3. Measurements were performed at least three random areas per sample.

Automatic goniometer CAM200 (KSV Inc., Finland) was used to measure the water contact angles on the surfaces by static sessile drop method. Ultrapure water was used as a probe liquid, and the measurements were carried out in air at room temperature. For each type of surface, at least three samples were measured to obtain a statistical result.

2.2. Cell isolation and culture

Human umbilical vein endothelial cells (HUVECs) were isolated from healthy human umbilical veins according to our previous method [16]. The obtained HUVECs were cultured in medium 199 (Hyclone), supplemented with 20% (v/v) bovine serum (Hyclone), 30 μg/mL endothelial cell growth supplement (ECGS) (Millipore), 1% (v/v) penicillin–streptomycin (Gibco) and 0.5% (v/v) heparin (medical grade), at 37 °C in 5% CO_2 atmosphere. The medium was changed every 3 days. When confluent, the cells were harvested with 0.05% (w/v) trypsin-0.02% (w/v) ethylenediaminetetraacetic acid (EDTA) solution. Passage 3–5 HUVECs were used in this study.

2.3. Cell morphology observation

HUVECs were seeded at a density of 2.5×10^4 cells/cm^2 on 96-well tissue culture polystyrene (TCPS) plates (Corning) with or without the bare and TiN-coated NiTi alloys and chitosan film samples (sample diameter 6 mm), and cultured in medium 199 containing 20% bovine serum and 1% penicillin–streptomycin for 4 h and 24 h, respectively. After each incubation period, the cell morphology was visualized by fluorescent acridine orange staining. In brief, all samples were rinsed with phosphate-buffered saline solution (PBS) (pH 7.4) once, and then cells were fixed with 95% (v/v) ethanol for 10 min, and incubated with 0.02% (w/v) acridine orange solution for 15 min at room temperature in darkness. After washing with PBS three times, the adherent cells were examined using a fluorescence microscope (BX51, Olympus, Japan).

2.4. Cell adhesion assay

HUVECs were seeded on TCPS dishes (Corning) with or without the bare and TiN-coated NiTi alloys and chitosan film samples (sample diameter 52 mm), at a density of 2.5×10^4 cells/cm^2 and cultured in medium 199 containing 20% bovine serum and 1% penicillin–streptomycin. After 2 or 4 h, medium was removed and surfaces were washed with PBS twice, adherent cells were collected by trypsinization and counted using a hemocytometer. Cell adhesion rate was calculated from the proportion of adherent/seeded cells.

2.5. Cell viability assay (MTT test)

HUVECs were cultured on the bare and TiN-coated NiTi alloys, chitosan film and TCPS for 4 and 24 h according to the procedure described in the cell morphology observation. After each incubation period, the cell viability was determined by methylthiazoltetrazolium (MTT) assay according to the method described in our previous study [21].

2.6. Serum proteins adsorption kinetics determination

Bare and TiN-coated NiTi alloys and chitosan film samples with 52 mm diameter were placed in TCPS dish separately. 5 mL medium 199 containing 20% bovine serum was added to each dish, and incubated at 37 °C in 5% CO_2 atmosphere for 0.25, 0.5, 1, 2, 3, 4 and 5 h, respectively. After each incubation period, the medium was removed and the samples were gently rinsed once in PBS to remove residual medium, and then samples were placed in new dishes to avoid interference from serum proteins adsorbed on TCPS. 1 mL buffer solution (8 M Urea, 0.1 M TrisBase, 0.01 M DTT, pH 8.6) was added to the surface of each samples, and incubated at room temperature for 20 min, to eluted adsorbed proteins from sample surface. All samples were eluted twice by the buffer solution. This could effectively remove the adsorbed proteins from the surfaces as determined by Fourier transform infrared (FTIR) spectroscopy analysis (Supplementary Fig. S1) and protein concentration measurement. Total protein concentration in the eluate was determined by the Bradford assay. At least triplicate samples for each type surface were measured at each time point to obtain a statistical result.

2.7. Proteomic analysis of adsorbed serum proteins

According to the procedure described in the serum proteins adsorption assay, the bare and TiN-coated NiTi alloys and chitosan film were incubated with medium 199 containing 20% bovine serum for 3 h, and then adsorbed proteins were collected by elution. For each type of surface, adsorbed proteins collected from fourteen independent samples were pooled to address biological variation and to obtain enough proteins for proteomic analysis. Protein samples were desalted by dialysis using membrane with a molecular weight cut off of 1000 Da, and concentrated by freeze-drying. The samples were separated by SDS-PAGE and subsequent identified by NanoLC-MS/MS peptide sequencing technology were performed in ProtTech, Inc., (Norristown, PA, USA). In brief, each gel was sliced into 20 fractions, and proteins in each slice were then digested in-gel with sequencing grade modified trypsin. The resulted peptides mixture was analyzed by a LC-MS/MS system, in which a high performance liquid chromatography (HPLC) with a 75 μm inner diameter reverse phase C18 column was on-line coupled with an ion trap mass spectrometer. The mass spectrometric data acquired were used to search the most recent non-redundant protein database with ProtTech's proprietary software suite. The output from the database search was manually validated to verify proper protein identification. Finally, relative protein abundance in each sample was obtained by label-free protein quantitation.

2.8. Bioinformatics analysis

Functional category and KEGG pathway analyses of identified proteins were performed by DAVID software (http://david.abcc.ncifcrf.gov/). RGD sequence distribution of the identified proteins was analyzed using ScanProsite software (http://prosite.expasy.org/scanprosite/).

2.9. Verification experiments

2.9.1. Intracellular calcium levels determination

According to the procedure described in the cell adhesion assay, HUVECs adhered on the bare and TiN-coated NiTi alloys and chitosan film after 0.5, 1, 2, 3 and 4 h culture were collected respectively by trypsinization. For the 0.5 h of culture, nonadherent cells were also collected because a major of seeded cells had not adhered at this time. To determine intracellular calcium levels, membrane permeable calcium indicator Fluo-3/AM (Beyotime, Haimen, China) was used according to the manufacturer's protocol. In brief, the collected cells were incubated with 5 μM Fluo-3/AM for 30 min at room temperature in darkness, and the fluorescent intensity of Fluo-3 was measured by flow cytometer (BD FACSCalibur, BD Biosciences, USA) with excitation and emission wavelengths of 488 and 525/530 nm, respectively.

2.9.2. Quantitative reverse transcriptase polymerase chain reaction (qRT-PCR)

Based on bioinformatics analyses, three transforming growth factor-beta (TGF-β) receptor isoform genes (*TGFBR*1, *TGFBR*2 and *TGFBR*3) in TGF-β signaling pathway, four important upstream genes (vinculin (*VCL*), talin 1 (*TLN*1), paxillin (*PXN*) and focal adhesion kinase (*FAK*)) [22] and one crucial downstream gene (serine/threonine kinase Akt, *AKT*) in focal adhesion pathway, and nine endothelial cell integrin α/β subunit genes (*ITGA*1, *ITGA*2, *ITGA*5, *ITGA*6, *ITGA*9, *ITGAV*, *ITGB*1, *ITGB*3 and *ITGB*5) [23] were selected for qRT-PCR analysis. HUVECs were seeded on the bare and TiN-coated NiTi alloys and chitosan film, and cultured for 4 and 24 h according to the procedure described in the cell adhesion assay. Total RNA was extracted using RNAiso plus (Takara, Dalian, China). The concentration and purity of RNA samples were measured using a UV/Vis spectrophotometer (Implen NanoPhotometer, Implen Corp., Germany). Complementary DNA (cDNA) was synthesized using PrimeScript reverse transcriptase kit (Takara, Dalian, China) for subsequent PCR amplification. Quantitative real-time PCR was performed on a 7500 Real-Time PCR system (Applied Biosystems Inc., USA) with SYBR real-time PCR kit (Takara, Dalian, China). Primers used in this study were listed in Supplementary Table S1. For each gene, the qRT-PCR analysis was repeated at three times. β-Actin was used as housekeeping reference gene because its threshold cycle value (Ct) did not differ significantly among samples (data not shown). Gene relative expression ratios were calculated using the $2^{-\Delta\Delta Ct}$ method [24], and the −ΔΔCt was calculated with the following formula, in which, cell cultured on the chitosan film was used as control.

$$-\Delta\Delta Ct = -\left[\left(Ct_{\text{target gene}} - Ct_{\text{actin}}\right)_{\text{test-material}} - \left(Ct_{\text{target gene}} - Ct_{\text{actin}}\right)_{\text{control}}\right] \quad (1)$$

2.9.3. Immunofluorescent staining of actin cytoskeleton and focal adhesion

HUVECs were cultured on the bare and TiN-coated NiTi alloys and chitosan film for 4 and 24 h according to the procedure described in the cell morphology observation. At the end of each culture period, actin cytoskeleton and focal adhesion of cells adhered on the above surfaces were stained using actin cytoskeleton and focal adhesion staining kit (Millipore, USA) according to the manufacturer's protocol. In brief, the adherent cells were fixed with 4% paraformaldehyde in 1× PBS for 20 min, permeabilized with 0.1% Triton X-100 in 1× PBS for 5 min and blocked with 1% BSA (Sigma) for 30 min. Then the cells were incubated with vinculin monoclonal antibody (1:300) for 1 h. After washing three times (5 min each) with 1× wash buffer, the cells were incubated with FITC conjugated goat anti-mouse IgG (1:125) and TRITC-conjugated phalloidin (1:250) for 50 min. The cells were then washed three times (5 min each) with 1× wash buffer, and nucleus staining was performed by incubating with DAPI (1:1000) for 4 min. The stained cells were examined using a fluorescence microscope (BX51, Olympus, Japan).

2.10. Statistical analysis

Data were presented as mean values ± standard deviation. Statistical analysis was performed using SPSS 15.0 software. Statistical significance was measured using one way analysis of variance (ANOVA) followed by Student–Newman–Keuls or Dunnett C post-hoc tests for all paired combinations, and the mean difference was considered to be significant while p value < 0.05, and very significant while p value < 0.01.

3. Results

3.1. Surface roughness and contact angle

The AFM images (Fig. 1a–c) show that the TiN-coated NiTi alloy had smoother surface than the bare NiTi alloy and chitosan film. Surface roughness measurement (Fig. 1d) demonstrated that the TiN-coated NiTi alloy had a lower Rms value of 1.5 ± 0.1 nm, whereas the bare NiTi alloy and chitosan film exhibited higher Rms value of 5.5 ± 0.3 nm, 2.8 ± 0.4 nm, respectively. As shown in Fig. 1e, the water contact angle of the TiN-coated NiTi alloy was significantly smaller than the bare NiTi alloy and chitosan film, suggesting that the TiN-coated NiTi alloy was more hydrophilic than the bare NiTi alloy and chitosan film.

3.2. Cell morphology, adhesion and viability

Fig. 2a shows cell morphology of HUVECs on the bare and TiN-coated NiTi alloys, chitosan film and TCPS after 4 h and 24 h of culture. Similar cell shape and spreading was observed on the alloys and TCPS at both 4 h and 24 h. In comparison, cells cultured on the chitosan film spread less and exhibited round shape at 4 h. Fig. 2b shows adhesion rate of HUVECs on the four types of surface. After 2 h incubation, the adherent cells on the alloys were significantly higher than those on the chitosan film and TCPS. After 4 h of culture, cells adhered to the four surfaces were all increased and TiN-coated NiTi alloy almost reached a complete cell adhesion. However, cell adhesion on the chitosan film and TCPS was still lower than the alloys. Cell viability evaluated by MTT method is shown in Fig. 2c. The cell viability on the bare and TiN-coated NiTi alloys and TCPS was significantly higher than that on the chitosan film at 4 h. After 24 h of culture, the cell viability on the bare and TiN-coated NiTi alloys was significantly higher than the chitosan film and TCPS, however, there was no obvious difference between the chitosan film and TCPS. These results indicated that the bare and TiN-coated NiTi alloys were much more suitable for HUVECs adhesion and growth than the chitosan film.

3.3. Protein adsorption kinetics

The adsorption kinetics of serum proteins on the bare and TiN-coated NiTi alloys and chitosan film is shown in Fig. 3. The protein adsorption amount on the bare and TiN-coated NiTi alloys was higher than that on the chitosan film at different incubation time except for the first 30 min. For the bare and TiN-coated NiTi alloys, the serum protein adsorption curves presented similar trend, the protein adsorption gradually increased within 1 h, then decreased at 2 h, and finally reached equilibrium at 3 h. For the chitosan film, an initial fast adsorption over the first 30 min was observed, and

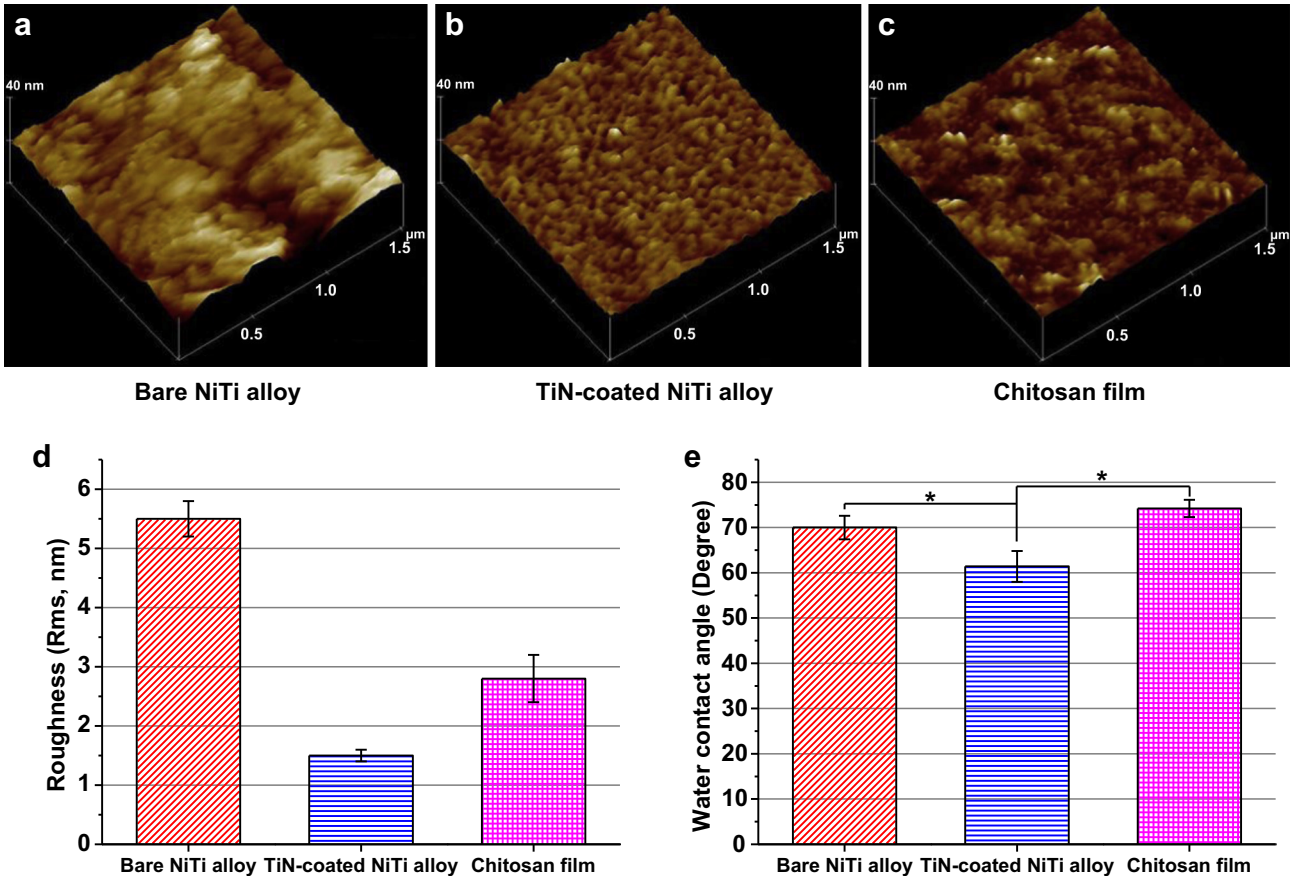

Fig. 1. AFM characterization and contact angle measurement. AFM images for (a) bare NiTi alloy, (b) TiN-coated NiTi alloy and (c) chitosan film sample surfaces. (d) Surface roughness (Rms) and (e) water contact angle value for the alloys and the chitosan film. Each value is the mean ± standard deviation of triplicate determinations; $^{*}p < 0.05$.

then protein adsorption was sharply reduced and maintained at a relatively stable level. Although the alloys and the chitosan film exhibited different protein adsorption kinetic curve, the protein adsorption on the bare and TiN-coated NiTi alloys and chitosan film all got equilibrium at 3 h with a total protein adsorption amount of 10.8 μg/cm^2, 11.22 μg/cm^2 and 7.93 μg/cm^2, respectively.

3.4. Proteomics results

The results of proteomic analysis showed that 111, 110 and 86 serum proteins adsorbed on the bare NiTi alloy, TiN-coated NiTi alloy and chitosan film, respectively, of which 68 proteins commonly adsorbed on the three surfaces. The type of proteins individually adsorbed was 43 for bare NiTi alloy, 42 for TiN-coated NiTi alloy and 18 for chitosan film (Table 1). Detailed information and relative abundance value of the commonly and individually adsorbed proteins were shown in Supplementary tables (Tables S2–S5).

3.5. Bioinformatics analyses

3.5.1. Functional category analysis

Functional category analysis showed that the identified proteins on the bare NiTi alloy, TiN-coated NiTi alloy and chitosan film involved in 31, 31 and 26 enriched functional categories, respectively. Among them, 24 categories (such as secreted, signal, glycoprotein and so on) were common for the identified proteins on the three surfaces (Supplementary Tables S6).

3.5.2. Biological pathways analysis

Biological pathway analysis showed that the identified proteins on the bare and TiN-coated NiTi alloys and chitosan film linked to a total of 24 KEGG biological pathways (Supplementary Table S7). Five biological pathways could be activated by binding of the identified proteins as ligands to cell surface receptors. Fig. 4a lists four biological pathways related to at least two surfaces and displays six proteins that activate these pathways. In the four pathways, two adsorbed proteins on the bare NiTi alloy, and one adsorbed proteins on the TiN-coated NiTi alloy and the chitosan film participated in activation of adipocytokine signaling pathway. For TGF-β signaling pathway, one adsorbed protein, thrombospondin 1 (THBS1) on the bare and TiN-coated NiTi alloys participated in activation of it, while no adsorbed protein on the chitosan film could activate the pathway. Three adsorbed proteins on the alloys and two adsorbed proteins on the chitosan film participated in activation of focal adhesion pathway. Moreover, two adsorbed proteins on the three surfaces participated in activation of regulation of actin cytoskeleton pathway. As seen from Fig. 4a, THBS1 participated in activation of TGF-β signaling and focal adhesion pathways, and fibronectin 1 (FN1) activated focal adhesion and regulation of actin cytoskeleton pathways.

Fig. 4b shows the relative abundance and amount of the six proteins, which activate the above four biological pathways, on the three surfaces. With the exception of vitronectin (VTN), the other five proteins including adiponectin (ADIPOQ), coagulation factor II (F2), FN1, THBS1 and leptin (LEP) exhibited higher relative abundance and amount on the bare and TiN-coated NiTi alloys than

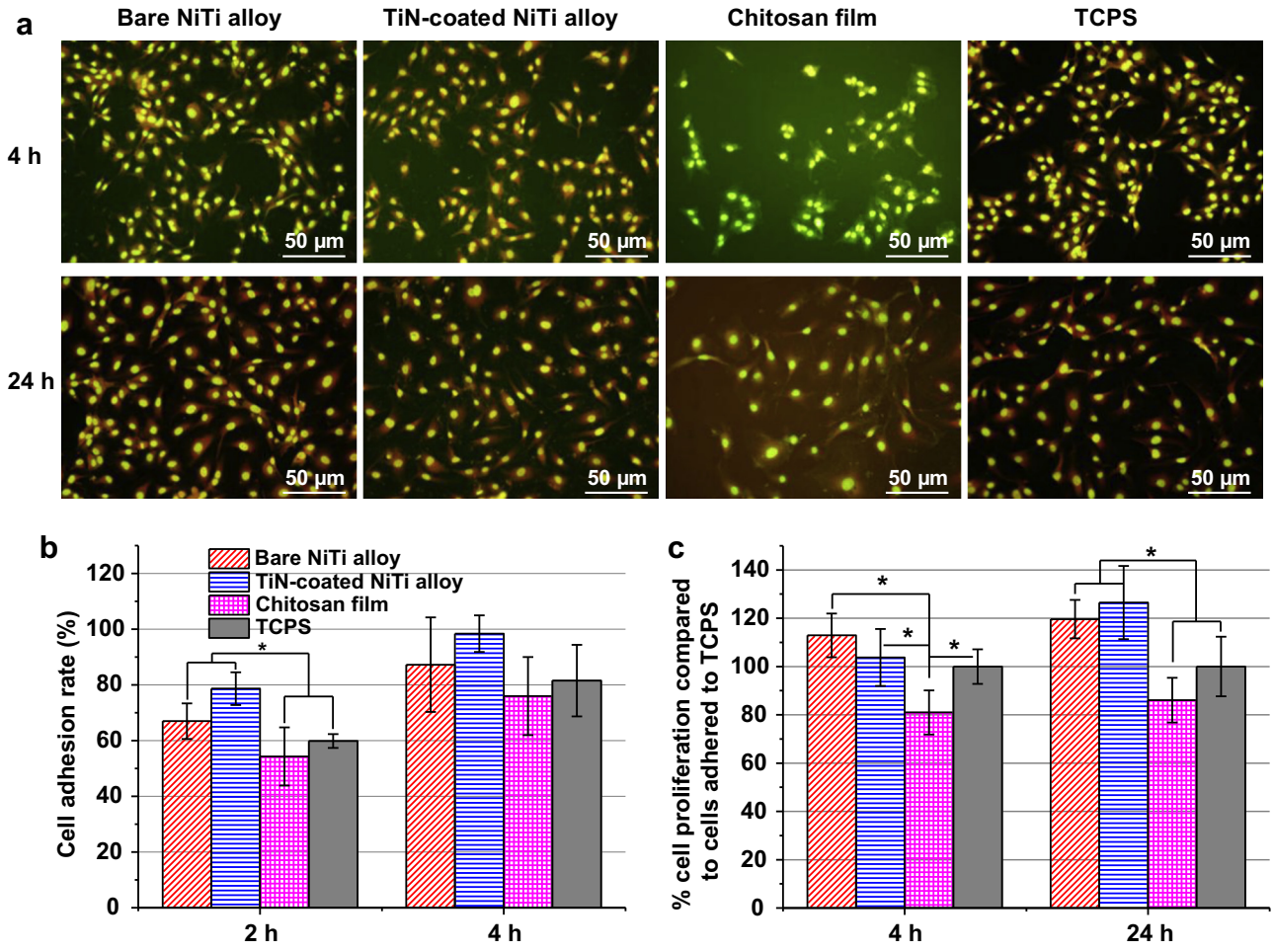

Fig. 2. HUVECs morphology, adhesion and viability on bare and TiN-coated NiTi alloys, chitosan film and TCPS. (a) Morphology of HUVECs on these samples after 4 h and 24 h culture was visualized by fluorescent acridine orange staining. (b) Adhesion rate of HUVECs on the four samples after 2 h and 4 h culture was obtained by calculation the proportion of adherent/seeded cells. (c) Viability of HUVECs on these samples after 4 h and 24 h culture was assayed by MTT method. Each value is the mean ± standard deviation of triplicate determinations; $^{*}p < 0.05$.

those on the chitosan film. As illustrated in Fig. 4c, three proteins, FN1, THBS1 and VTN could bind to cell surface integrins, and activate the focal adhesion pathway.

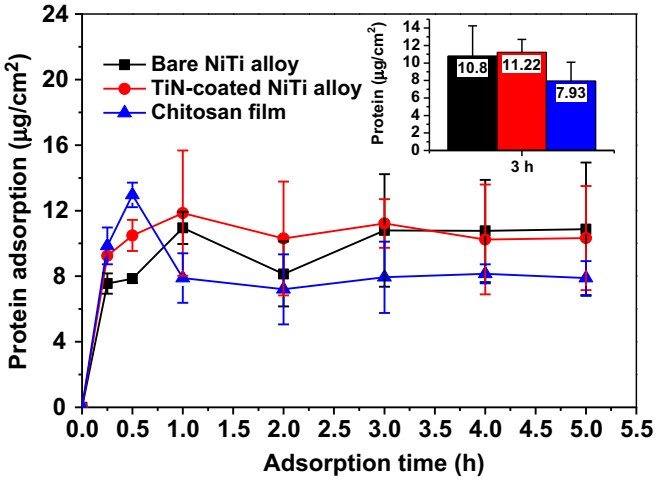

Fig. 3. Protein adsorption onto the bare and TiN-coated NiTi alloys and chitosan film after incubated with medium 199 containing 20% bovine serum for different time. Each value is the mean ± standard deviation of triplicate determinations.

3.5.3. RGD sequence distribution analysis

The RGD sequence distribution of identified proteins on bare NiTi alloy, TiN-coated NiTi alloy and chitosan film is shown in Table 2. Seven proteins containing RGD sequence (FN1, F2, CFH, VTN, SERPINF2, THBS1 and FBLN1) were identified on the bare and TiN-coated NiTi alloys, whereas only five proteins containing RGD sequence (FN1, F2, CFH, VTN and SERPINF2) were identified on the chitosan film. Moreover, the relative abundance and amount of FN1, F2 and CFH on the bare and TiN-coated NiTi alloys were much higher than that on the chitosan film.

3.6. Verification experiments

3.6.1. Intracellular calcium levels

Fig. 5 shows the intracellular free calcium concentrations in HUVECs after cultured on the bare NiTi alloy, TiN-coated NiTi alloy

Table 1
Types of proteins adsorbed on bare and TiN-coated NiTi alloys and chitosan film.

Samples	Type of adsorbed proteins		
	Total	Common	Individual
Bare NiTi alloy	111	68	43
TiN-coated NiTi alloy	110		42
Chitosan film	86		18

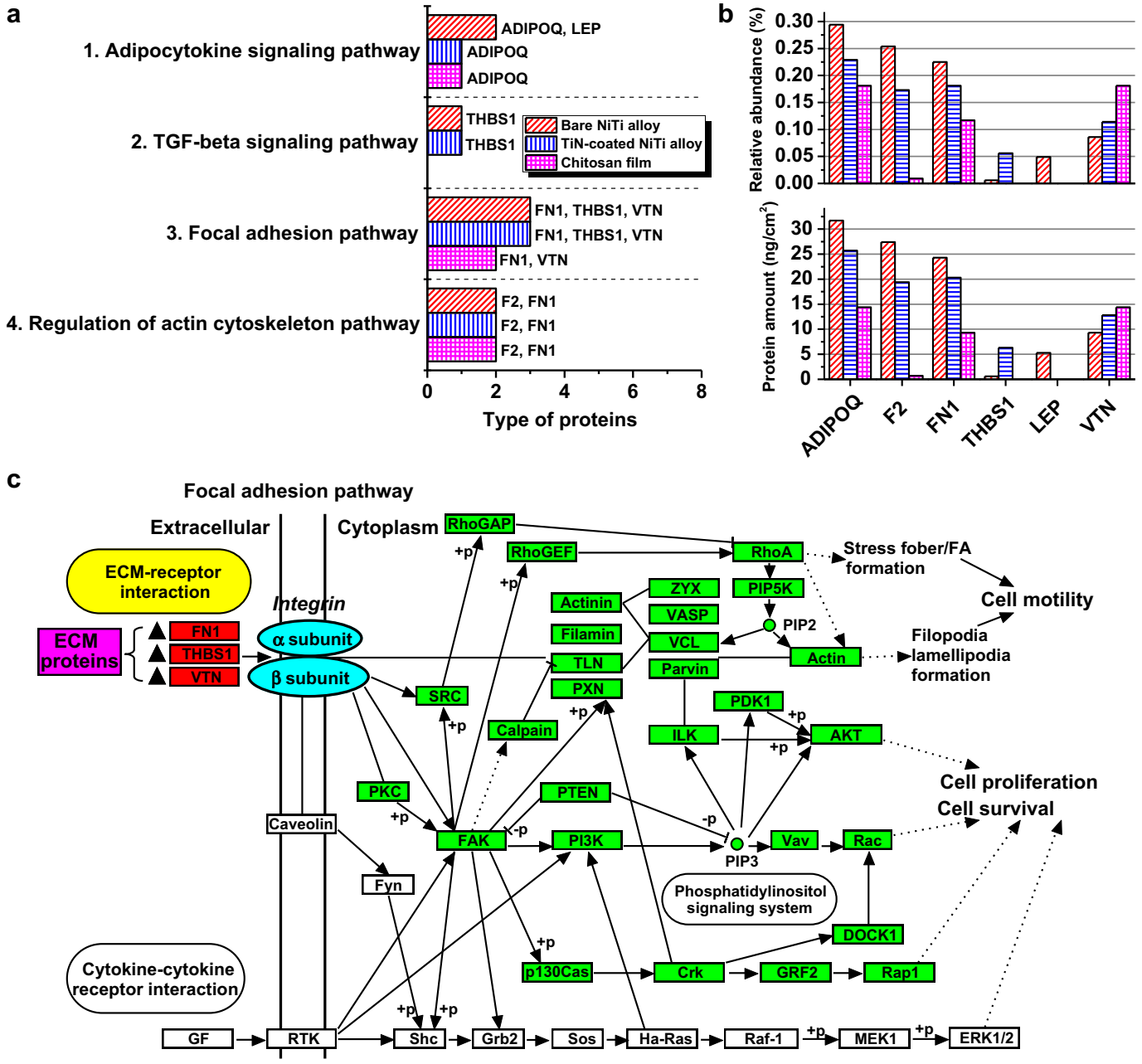

Fig. 4. (a) Four concerned KEGG pathways that could be activated by binding of the identified proteins as ligands to cell surface receptors. (b) Relative abundance and amount for six identified proteins, which activate the four biological pathways, on the bare and TiN-coated NiTi alloys and chitosan film. Protein amount = relative abundance value × total protein adsorption amount. The total protein adsorption at per square centimeter was 10.8 μg for bare NiTi alloy, 11.22 μg for TiN-coated NiTi alloy and 7.93 μg for chitosan film. (c) Graphical presentation of focal adhesion pathway obtained from KEGG database with some modification. ▲, the adsorbed proteins identified in this study.

and chitosan film for different times. The maximum intracellular calcium concentration values for HUVECs on the bare and TiN-coated NiTi alloys were observed after 0.5 h of culture, while chitosan film showed the maximum intracellular calcium concentration after 1 h of culture. After that, the intracellular calcium levels on these three surfaces decrease with culture time. It indicated that the calcium peaks in HUVECs cultured on the bare and TiN-coated NiTi alloys reached earlier than that on the chitosan film.

3.6.2. *Relative expression of TGF-β pathway and focal adhesion pathway genes and integrin α/β subunit genes*

Fig. 6a–c shows the relative expression of three TGF-β pathway genes (*TGFBR*1, *TGFBR*2 and *TGFBR*3), five focal adhesion pathway genes (*VCL*, *TLN*1, *PXN*, *FAK* and *AKT*) and nine integrin α/β subunit genes (*ITGA*1, *ITGA*2, *ITGA*5, *ITGA*6, *ITGA*9, *ITGAV*, *ITGB*1, *ITGB*3 and *ITGB*5) in HUVECs cultured on bare and TiN-coated NiTi alloys and chitosan film for 4 h and 24 h, respectively. For these 17 genes, the expression of 16 genes except the integrin α subunit gene *ITGA*1 in HUVECs cultured on the bare and TiN-coated NiTi alloys were all significantly ($p < 0.05$) or very significantly ($p < 0.01$) higher than that on the chitosan film. In particular, after the culture of 4 h, the relative expression of TGF-β receptor type 3 (*TGFBR*3) and paxillin (*PXN*) was up-regulated on the TiN-coated NiTi alloy by approximate 143 and 1391 fold, respectively (Fig. 6a and b). The integrin subunit genes *ITGA*5, *ITGA*6 and *ITGB*5 up-regulated on the TiN-coated NiTi alloy by approximate 91, 36 and 57 fold, respectively (Fig. 6c).

Table 2
RGD sequence distribution of the identified proteins was obtained by ScanProsite analysis.

No.	UniProt accession	Protein name (symbol)	RGD location	Relative abundance (%)			Protein amount (ng/cm^2)[a]		
				NiTi	TiN–NiTi	Chitosan	NiTi	TiN–NiTi	Chitosan
1	P07589	Fibronectin 1 (FN1)	1616–1618 2183–2185	0.225	0.181	0.117	24.3	20.3	9.3
2	P00735	Coagulation factor II (F2)	563–565	0.254	0.173	0.009	27.4	19.4	0.7
3	Q3ZBS7	Vitronectin (VTN)	64–66 128–130	0.086	0.114	0.181	9.3	12.8	14.4
4	P28800	Alpha-2-antiplasmin (SERPINF2)	466–468	0.018	0.033	0.045	1.9	3.7	3.6
5	Q28085	Complement factor H (CFH)	246–248	0.067	0.072	0.006	7.2	8.1	0.5
6	Q28178	Thrombospondin 1 (THBS1)	926–928	0.006	0.056	ND	0.6	6.3	ND
7	A5D7S8	Fibulin 1 (FBLN1)	95–97	0.015	0.003	ND	1.6	0.3	ND

[a] Protein amount = relative abundance value × total protein adsorption amount. The total protein adsorption at per square centimeter was 10.8 μg for bare NiTi alloy, 11.22 μg for TiN-coated NiTi alloy and 7.93 μg for chitosan film. ND: not detected.

3.6.3. Actin cytoskeleton and focal adhesion observation

Fig. 7 shows the actin cytoskeleton and focal adhesion in HUVECs cultured on bare and TiN-coated NiTi alloys and chitosan film for 4 h and 24 h. Distinct difference in actin cytoskeleton organization and focal adhesion formation was observed between the alloys and the chitosan film. Well organized actin cytoskeleton fibers (red color) and obvious focal adhesions marked by dot-like vinculin (green color) were detected in the HUVECs cultured on the bare and TiN-coated NiTi alloys at 4 h (Fig. 7a and b). In contrast, cells grew on the chitosan film were almost round shape, meanwhile, the actin cytoskeleton fibers and focal adhesions were vague (Fig. 7c). Although cells spread on the chitosan film after 24 h culture, the focal adhesions were still not obvious (Fig. 7f). In comparison, apparent actin cytoskeleton fibers and focal adhesions were observed in cells grew on the bare NiTi alloy, especially on the TiN-coated NiTi alloy (Fig. 7d and e). These results indicated that the bare and TiN-coated NiTi alloys could promote actin cytoskeleton organization and focal adhesion formation compared to the chitosan film.

4. Discussion

The different endothelial cell adhesion, spreading and viability on the alloys and chitosan film might result from different serum proteins adsorption. To explore the mechanism of mediation of adsorbed protein layer to endothelial cell behavior, this study investigated the components of adsorbed serum proteins by proteomic analysis. Since proteins adsorption on material surface is an adsorption/desorption process, it is necessary to pre-determine an appropriate protein's incubation time. Serum proteins adsorption on the three materials basically did not change after 3 h incubation (Fig. 3), indicating that constant interchanges of adsorbed proteins at these surfaces, i.e., the Vroman effect [25]. Hence, 3 h was selected as protein's incubation time in proteomic analysis.

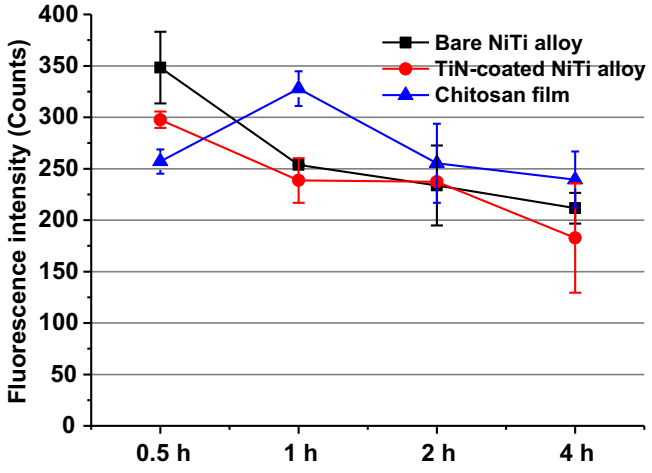

Fig. 5. Intracellular calcium levels in HUVECs after cultured on bare and TiN-coated NiTi alloys and chitosan film for different times were determined using membrane permeable calcium indicator Fluo-3/AM. Each value is the mean ± standard deviation of triplicate determinations.

Cell adhesion is accomplished by adhesion receptors such as integrins, immunoglobulin superfamily, cadherins and selectins where integrins are predominantly receptors to mediate cell adhesion on extracellular matrix (ECM). Integrins are α-β heterodimers, which can bind to ECM component through its extracellular region, and link cytoplasmic protein complexes including vinculin (VCL), talin (TLN), paxillin (PXN) and focal adhesion kinase (FAK) through its intracellular region to constitute site of anchorage of actin cytoskeletons [22]. Binding of integrin with extracellular ligands activates focal adhesion signaling pathway, which can increase formation of focal adhesions, regulate actin cytoskeleton structure, and promote cell adhesion and spreading [26]. However, integrins are normally expressed on cell surface in an inactive state, and unable to bind to their ligands until they are activated by stimulating signals from other receptors [27]. Therefore, the integrin-mediated cell adhesion should be at least dependent on three aspects, the activation of cell surface integrins, integrin expression and integrin ligand proteins adsorbed on biomaterials.

Previous studies have demonstrated that binding of several types of cell surface receptor with extracellular ligand proteins could activate cell surface integrins through signal transduction [27,28]. Among these activation pathways, the increase of intracellular calcium concentration is a common early step and the binding of TLN to the tail of integrin-β subunits in cytoplasm is a common final step. In this study, the type of signal-related proteins adsorbed on the bare and TiN-coated NiTi alloys (47 and 46 proteins) was obviously more than the chitosan film (36 proteins) (Supplementary Table S6). The amount of adsorbed proteins (such as ADIPOQ), which could activate signaling pathways, on the alloys was also more than chitosan film (Fig. 4a and b and Supplementary Fig. S2). These indicated that the adsorbed proteins on the alloys might trigger more signaling transduction compared to chitosan film. Binding of ADIPOQ with cell surface ADIPOQ receptor has been reported to activate signaling pathway though increasing intracellular calcium level [29,30]. In this study, the calcium peaks of HUVECs on the alloys reached earlier than chitosan film (Fig. 5). Since cytosolic calcium ion is a versatile cell second messenger, the increase of intracellular calcium level indicates stronger cell signal transduction, which verified the proteomic analysis results. The expression of *TLN* 1 in HUVECs on the alloys at 4 h was significantly higher than chitosan film (Fig. 6b). The earlier increase

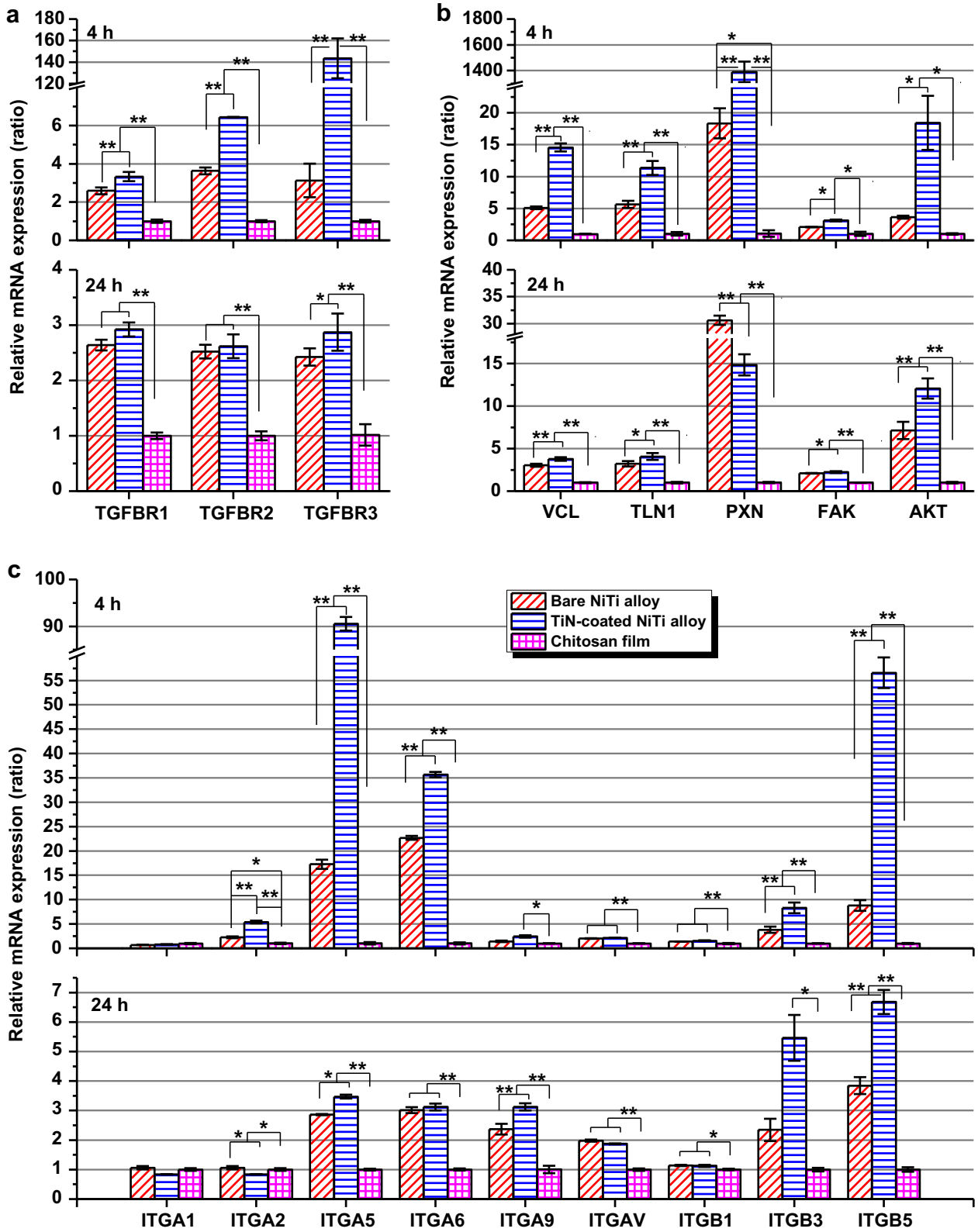

Fig. 6. Relative expression of (a) TGF-β pathway genes, (b) focal adhesion pathway genes, and (c) integrin α/β subunit genes in HUVECs cultured on bare and TiN-coated NiTi alloys and chitosan film were assessed by qRT-PCR after 4 and 24 h of culture. β-Actin was used as housekeeping reference gene. Cell cultured on chitosan film was set as control. Each value is the mean ± standard deviation of triplicate determinations; $^{*}p < 0.05$, $^{**}p < 0.01$.

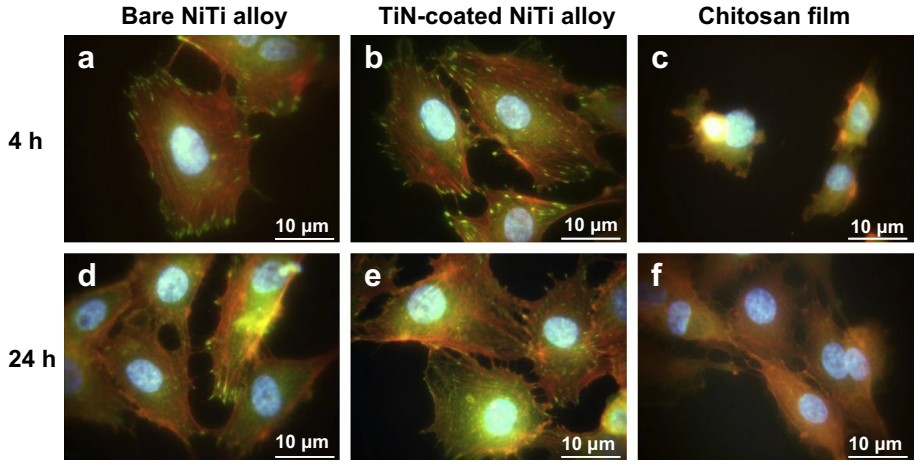

Fig. 7. Fluorescence microscope images of HUVECs cultured on bare and TiN-coated NiTi alloys and chitosan film for 4 h and 24 h. Actin cytoskeleton, focal adhesion and cell nuclei in HUVECs were visualized by immunofluorescent staining of actin filaments (red), vinculin (green) and nucleus (blue), respectively. (For interpretation of the references to color in this figure legend, the reader is referred to the web version of this article.)

of intracellular calcium concentration and higher expression of *TLN* 1 in HUVECs on the alloys could result in stronger activation of cell surface integrins.

Meanwhile, the adsorbed THBS1 on the alloys participated in activating TGF-β signaling pathway, while no adsorbed proteins on chitosan film participated in activating the pathway (Fig. 4a and Supplementary Fig. S3). THBS1 could active TGF-β and allow it to bind with cell surface TGF-β receptors (TGFBR1 and TGFBR2), which result in TGF-β signaling pathway activation [31]. TGFBR3 is a major accessory receptor promoting TGF-β ligand binding to its receptors [32]. The expressions of *TGFBR*1 and *TGFBR*2, especially *TGFBR*3 in HUVECs on the alloys were significantly higher than chitosan film (Fig. 6a), suggesting TGF-β pathway might be activated in HUVECs on the alloys.

Existing reports have demonstrated that activated TGF-β signaling pathway could enhance integrin expression to regulate cell adhesion, such as increasing integrin subunit *ITGB*1 expression to stimulate human osteosarcoma cells adhesion on FN [33], up-regulating integrin subunits *ITGA*2, *ITGA*6 and *ITGB*1 expression to promote human mesenchymal stem cells adhesion on type I collagen [34], and augmenting integrin subunit *ITGB*5 expression to increase osteoblast-like cells adhesion on vitronectin [35]. In the study, the expression of integrin α/β subunit genes including *ITGA*2, *ITGA*9, *ITGAV*, *ITGB*1 and *ITGB*3, especially *ITGA*5, *ITGA*6 and *ITGB*5 were significantly up-regulated by the alloys as compared to chitosan film at 4 h, but decreased at 24 h (Fig. 6c). Usually, cultured cells could complete their adhesion on material surface within 4 h, and then begin to proliferate and migrate. Therefore, the expression of cell adhesion related genes dropped dramatically between 4 h and 24 h.

Three adsorbed proteins (FN1, VTN and THBS1) on the alloys and two adsorbed proteins (FN1 and VTN) on chitosan film participated in activating focal adhesion pathway through ECM-receptor interaction (Fig. 4a and c). Compared with chitosan film, the alloys significantly increased adsorption of FN1 and THBS1, but slightly decreased VTN adsorption (Fig. 4b). FN and VTN were able to promote cell adhesion on biomaterials where FN had greater ability than VTN [36,37]. It can be deduced that the influence of the three adsorbed proteins on focal adhesion pathway would be greater on the alloys than chitosan film.

RGD in adhesive proteins (such as FN) is a major recognition sequence required for cell surface integrins binding to these proteins. Cell adhesion on material surface can be triggered after integrins recognized and bound with RGD of adsorbed proteins [38]. If adsorbed protein contains RGD, it may promote cell adhesion. To further investigate the effect of adsorbed protein on cell adhesion, this study investigated RGD distribution of the identified proteins. The adsorption of RGD containing proteins on the alloys (7 proteins) was more than chitosan film (5 proteins), suggesting more integrin ligand proteins are available on the alloys.

Above all, by the mediation of adsorbed proteins, stronger activation and higher expression of integrins, as well as more available ligands for integrin will activate more integrin-mediated focal adhesion pathway in HUVECs on the alloys than chitosan film. As expected, expression of focal adhesion pathway genes (*VCL*, *TLN*, *PXN* and *FAK*) on the alloys was significantly higher than chitosan film. Furthermore, corresponding higher expression of downstream gene *AKT* was also detected (Fig. 6b).

F2 and FN1 adsorbed on the three surfaces could activate regulation of actin cytoskeleton pathway through binding with cell surface F2 receptor and integrin, respectively (Fig. 4a and Supplementary Fig. S4). Binding of F2 with its receptor increased actin stress fiber formation and regulated actin cytoskeleton organization [39]. As an adhesive protein, binding of FN1 with integrin not only promoted cell adhesion, but also increased actin stress fiber formation [40]. The amount of F2 and FN1 adsorbed on the alloys was higher than chitosan film, so the activation of adsorbed proteins to regulation of actin cytoskeleton pathway was greater on the alloys than chitosan film. As expected, expression of regulation of actin cytoskeleton pathway genes (*VCL*, *PXN* and *FAK*) in HUVECs on the alloys was significantly higher than chitosan film, suggesting stronger activation of the pathway. As seen from Fig. 4a and c and Supplementary Fig. S4, FN1 participated in activation of focal adhesion and regulation of actin cytoskeleton pathways. The two pathways were correlated with cell adhesion, which was an important reason for FN1 to promote cell adhesion.

The activated focal adhesion and regulation of actin cytoskeleton pathways will increase focal adhesion formation and regulate actin cytoskeleton structure. As expected, well arranged actin cytoskeleton fibers and numerous focal adhesions were observed in HUVECs on the alloys, while the actin cytoskeleton fibers and focal adhesions were vague in HUVECs on chitosan film (Fig. 7). The activation of focal adhesion pathway will not only increase cell adhesion, but also enhance cell survival and proliferation (Fig. 4c). This explains the better endothelial cell adhesion and growth on the alloys other than chitosan film (Fig. 2).

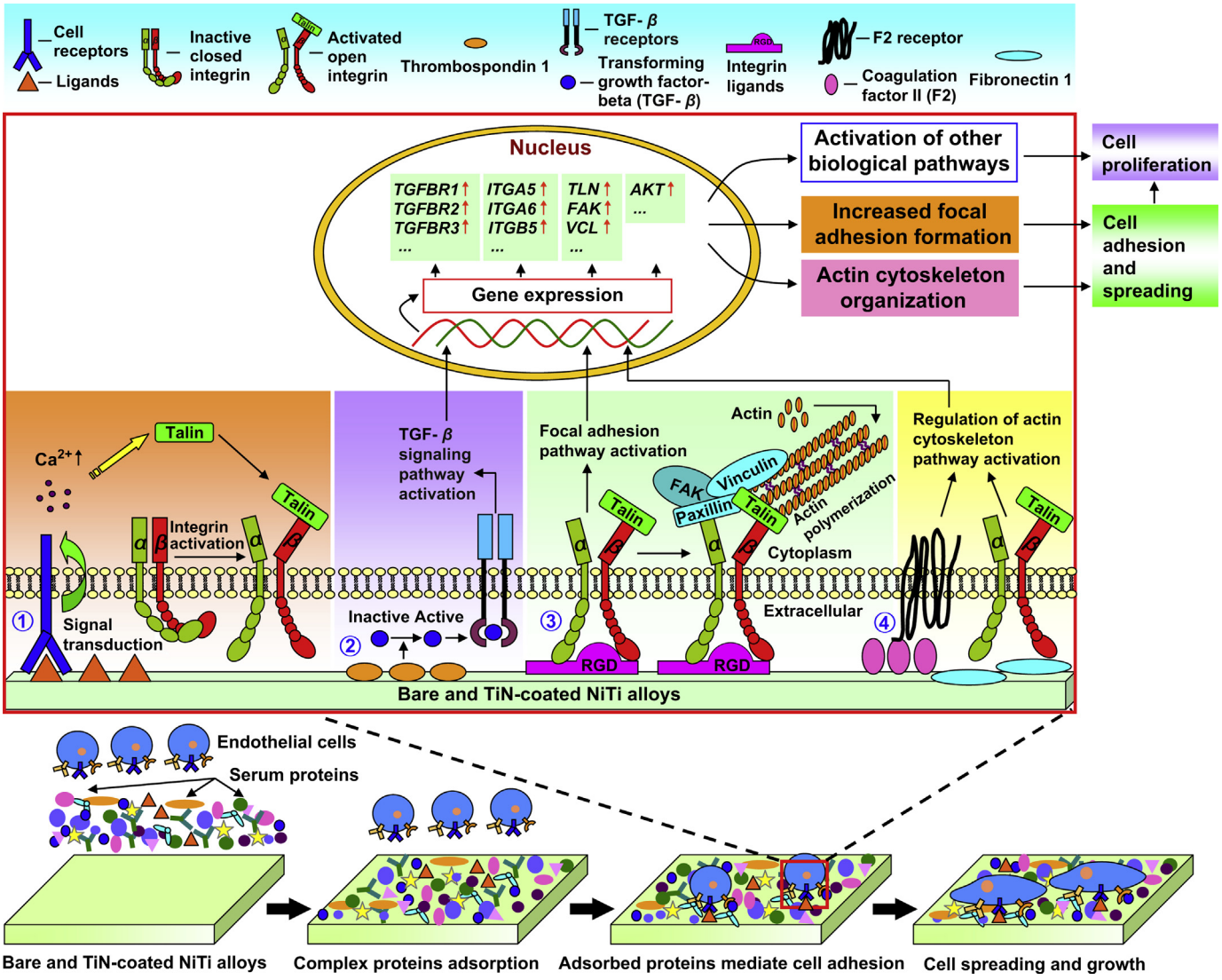

Fig. 8. Schematic diagram of mechanism of mediation of adsorbed protein layer components to endothelial cells adhesion and growth on bare and TiN-coated NiTi alloys.

Surface properties including surface roughness, wettability and surface chemistry play important roles in protein adsorption on biomaterials [41–43]. Bare NiTi alloy and chitosan film had larger surface roughness than TiN-coated NiTi alloy. However, the total protein adsorption on the alloys was higher than chitosan film. It was reported that nanoscale surface could affect protein adsorption and conformation [41], while surface roughness between 2 and 21 nm would not alter protein adsorption amount [44]. Although the surface roughness of the three materials was different, they were all below 6 nm (Fig. 1d). Therefore, the effect of surface roughness on protein adsorption amount could be neglected. Furthermore, a hydrophobic material surface was usually believed to tend to adsorb more protein than a hydrophilic material surface, however this would not affect the alloys and chitosan film. The chitosan film with a higher surface hydrophobicity (Fig. 1e) had lower serum proteins adsorption than the alloys (Fig. 3). Similar result was also reported by Allen et al., that the amount of serum proteins adsorbed on N-isopropylacrylamide-based co-polymer films decreased with increasing surface hydrophobicity [4]. There may be two reasons for this phenomenon of serum proteins adsorption. Firstly, serum contains many kinds of proteins, and different proteins may have different adsorption trends. It has been revealed that fibronectin showed greater adsorption on hydrophilic surfaces, whereas albumin predominantly adsorbed on hydrophobic surfaces [42]. Secondly, surface chemistry may play more important role in protein adsorption here. As reported by Clarke et al., surface roughness and hydrophobicity almost had no effect on albumin adsorption on NiTi alloy, while a clear correlation between surface nickel and oxygen concentration and amount of albumin adsorbed was observed [43]. In addition, chitosan, a pH-responsive polycation due to its primary amine present in glucosamine residue, may affect proteins adsorption under a small change in environmental pH [20]. Therefore, the decreased proteins adsorption on chitosan film may result from the effect of chemical groups such as amino group in chitosan.

It is known, protein conformation plays an important role in protein function. The conformation will change after protein adsorbed on material surface [45], and thereby, protein conformation is one of important scientific issue in study of protein adsorption. Although circular dichroism spectropolarimetry, Fourier transform infrared spectroscopy, and molecular simulation have been used in investigating conformation of single protein adsorbed on materials [45–47], the study of conformation of adsorbed protein layer components is lacking because of the limitation of tools

and the complexity of protein conformation. In the future, the mediation of adsorbed serum proteins to cell behavior can be better understood by proteomic analysis combined with protein conformation study.

5. Conclusions

This study found the adsorbed serum proteins on the alloys mediated endothelial cell adhesion and growth mainly via four ways. First, proteins such as adiponectin in the adsorbed protein layer bind with cell surface receptors to generate cell signal transduction, which activate cell surface integrins through increasing intracellular calcium level. Another way, thrombospondin 1 (THBS1) in the adsorbed protein layer promotes TGF-β signaling pathway activation and increases expression of integrins α/β subunit genes. The third, binding of RGD sequence containing proteins such as fibronectin 1 (FN1), vitronectin and THBS1 in the adsorbed protein layer with activated integrins activates focal adhesion pathway, increases focal adhesion formation and actin cytoskeleton organization, and leads to cell adhesion and spreading. The activated focal adhesion pathway also increases expression of cell growth related gene (such *AKT*), activates other biological pathways and promotes cell proliferation. The fourth route, coagulation factor II (F2) and FN1 in the adsorbed protein layer binds with cell surface F2 receptor and integrin, activates the regulation pathway of actin cytoskeleton and regulates actin cytoskeleton organization (Fig. 8). In addition, THBS1 and FN1, which contain RGD sequence and participate in activating two pathways, might play more important role in mediating cell adhesion and growth than other adsorbed proteins. This study elementarily reveals the molecular mechanism of mediation of adsorbed serum protein layer components to endothelial cell adhesion and growth on bare and TiN-coated NiTi alloys, this help to provide new insight in comprehension of biomaterial–protein–cell interactions.

Acknowledgments

This paper was supported by 973 Project (No. 2009CB930000), the National Natural Science Foundation of China (Nos. 31271012, 31170910), and the Specialized Research Fund for the Doctoral Program of Higher Education of China (No. 20100092110027).

Appendix A. Supplementary data

Supplementary data related to this article can be found at http://dx.doi.org/10.1016/j.biomaterials.2013.04.028.

References

[1] Castner DG, Ratner BD. Biomedical surface science: foundations to frontiers. Surf Sci 2002;500:28–60.
[2] Wilson CJ, Clegg RE, Leavesley DI, Pearcy MJ. Mediation of biomaterial–cell interactions by adsorbed proteins: a review. Tissue Eng 2005;11:1–18.
[3] Lord MS, Cheng B, McCarthy SJ, Jung M, Whitelock JM. The modulation of platelet adhesion and activation by chitosan through plasma and extracellular matrix proteins. Biomaterials 2011;32:6655–62.
[4] Allen LT, Tosetto M, Miller IS, O'Connor DP, Penney SC, Lynch I, et al. Surface-induced changes in protein adsorption and implications for cellular phenotypic responses to surface interaction. Biomaterials 2006;27:3096–108.
[5] Sask KN, Zhitomirsky I, Berry LR, Chan AKC, Brash JL. Surface modification with an antithrombin-heparin complex for anticoagulation: studies on a model surface with gold as substrate. Acta Biomater 2010;6:2911–9.
[6] Lü XY, Li DJ, Huang Y, Zhang YY. Application of a modified coomassie brilliant blue protein assay in the study of protein adsorption on carbon thin films. Surf Coat Technol 2007;201:6843–6.
[7] Huang Y, Lü XY, Qian WP, Tang ZM, Zhong YP. Competitive protein adsorption on biomaterial surface studied with reflectometric interference spectroscopy. Acta Biomater 2010;6:2083–90.
[8] Lü XY, Huang Y, Qian WP, Tang ZM, Lu ZH. An effective method for quantitative evaluation of proteins adsorbed on biomaterial surfaces. J Biomed Mater Res A 2003;66A:722–7.
[9] Anderson NL, Polanski M, Pieper R, Gatlin T, Tirumalai RS, Conrads TP, et al. The human plasma proteome – a nonredundant list developed by combination of four separate sources. Mol Cell Proteomics 2004;3:311–26.
[10] Derhami K, Zheng J, Li L, Wolfaardt JF, Scott PG. Proteomic analysis of human skin fibroblasts grown on titanium: novel approach to study molecular biocompatibility. J Biomed Mater Res 2001;56:234–44.
[11] Kaneko H, Kamiie J, Kawakami H, Anada T, Honda Y, Shiraishi N, et al. Proteome analysis of rat serum proteins adsorbed onto synthetic octacalcium phosphate crystals. Anal Biochem 2011;418:276–85.
[12] Huang L, Cao Z, Meyer HM, Liaw PK, Garlea E, Dunlap JR, et al. Responses of bone-forming cells on pre-immersed Zr-based bulk metallic glasses: effects of composition and roughness. Acta Biomater 2011;7:395–405.
[13] Hung HS, Wu CC, Chien S, Hsu SH. The behavior of endothelial cells on polyurethane nanocomposites and the associated signaling pathways. Biomaterials 2009;30:1502–11.
[14] Mukhatyar VJ, Salmeron-Sanchez M, Rudra S, Mukhopadaya S, Barker TH, Garcia AJ, et al. Role of fibronectin in topographical guidance of neurite extension on electrospun fibers. Biomaterials 2011;32:3958–68.
[15] Lai YX, Xie C, Zhang Z, Lu WY, Ding JD. Design and synthesis of a potent peptide containing both specific and non-specific cell-adhesion motifs. Biomaterials 2010;31:4809–17.
[16] Zhao LF, Hong Y, Yang DY, Lü XY, Xi TF, Zhang DY, et al. The underlying biological mechanisms of biocompatibility differences between bare and TiN-coated NiTi alloys. Biomed Mater 2011;6:025012.
[17] Jayakumar R, Prabaharan M, Nair SV, Tokura S, Tamura H, Selvamurugan N. Novel carboxymethyl derivatives of chitin and chitosan materials and their biomedical applications. Prog Mater Sci 2010;55:675–709.
[18] Silva SS, Luna SM, Gomes ME, Benesch J, Pashkuleva I, Mano JF, et al. Plasma surface modification of chitosan membranes: characterization and preliminary cell response studies. Macromol Biosci 2008;8:568–76.
[19] Lü XY, Cui W, Huang Y, Zhao Y, Wang ZG. Surface modification on silicon with chitosan and biological research. Biomed Mater 2009;4:044103.
[20] Chen Y-H, Chung Y-C, Wang IJ, Young T-H. Control of cell attachment on pH-responsive chitosan surface by precise adjustment of medium pH. Biomaterials 2012;33:1336–42.
[21] Lü XY, Bao X, Huang Y, Qu YH, Lu HQ, Lu ZH. Mechanisms of cytotoxicity of nickel ions based on gene expression profiles. Biomaterials 2009;30:141–8.
[22] Lo SH. Focal adhesions: what's new inside. Dev Biol 2006;294:280–91.
[23] Avraamides CJ, Garmy-Susini B, Varner JA. Integrins in angiogenesis and lymphangiogenesis. Nat Rev Cancer 2008;8:604–17.
[24] Livak KJ, Schmittgen TD. Analysis of relative gene expression data using real-time quantitative PCR and the 2(t)(-delta delta c) method. Methods 2001;25:402–8.
[25] Vroman L, Adams AL, Fischer GC, Munoz PC. Interaction of high molecular-weight kininogen, factor-XII, and fibrinogen in plasma at interfaces. Blood 1980;55:156–9.
[26] Carragher NO, Frame MC. Focal adhesion and actin dynamics: a place where kinases and proteases meet to promote invasion. Trends Cell Biol 2004;14:241–9.
[27] Anthis NJ, Campbell ID. The tail of integrin activation. Trends Biochem Sci 2011;36:191–8.
[28] Shattil SJ, Kim C, Ginsberg MH. The final steps of integrin activation: the end game. Nat Rev Mol Cell Biol 2010;11:288–300.
[29] Steyn FJ, Boehme F, Vargas E, Wang K, Parkington HC, Rao JR, et al. Adiponectin regulate growth hormone secretion via adiponectin receptor mediated Ca^{2+} signalling in rat somatotrophs in vitro. J Neuroendocrinol 2009;21:698–704.
[30] Buechler C, Wanninger J, Neumeier M. Adiponectin receptor binding proteins – recent advances in elucidating adiponectin signalling pathways. FEBS Lett 2010;584:4280–6.
[31] Lawler J. Thrombospondin-1 as an endogenous inhibitor of angiogenesis and tumor growth. J Cell Mol Med 2002;6:1–12.
[32] de Caestecker M. The transforming growth factor-beta superfamily of receptors. *Cytokine Growth F R* 2004;15:1–11.
[33] Nikitovic D, Chalkiadaki G, Berdiaki A, Aggelidakis J, Katonis P, Karamanos NK, et al. Lumican regulates osteosarcoma cell adhesion by modulating TGF beta 2 activity. Int J Biochem Cell Biol 2011;43:928–35.
[34] Warstat K, Meckbach D, Weis-Klemm M, Hack A, Klein G, de Zwart P, et al. TGF-beta enhances the integrin alpha 2 beta 1-mediated attachment of mesenchymal stem cells to type I collagen. Stem Cells Dev 2010;19:645–56.
[35] Lai CF, Feng X, Nishimura R, Teitelbaum SL, Avioli LV, Ross FP, et al. Transforming growth factor-beta up-regulates the beta(5) integrin subunit expression via sp1 and smad signaling. J Biol Chem 2000;275:36400–6.
[36] Danmark S, Finne-Wistrand A, Albertsson AC, Patarroyo M, Mustafa K. Integrin-mediated adhesion of human mesenchymal stem cells to extracellular matrix proteins adsorbed to polymer surfaces. Biomed Mater 2012;7:035011.
[37] Ku Y, Chung CP, Jang JH. The effect of the surface modification of titanium using a recombinant fragment of fibronectin and vitronectin on cell behavior. Biomaterials 2005;26:5153–7.

[38] Siebers MC, ter Brugge PJ, Walboomers XF, Jansen JA. Integrins as linker proteins between osteoblasts and bone replacing materials. A critical review. Biomaterials 2005;26:137–46.
[39] Ruiz-Loredo AY, Lopez E, Lopez-Colome AM. Thrombin promotes actin stress fiber formation in RPE through Rho/ROCK-mediated MLC phosphorylation. J Cell Physiol 2011;226:414–23.
[40] Chen XY, Su YD, Ajeti V, Chen SJ, Campagnola PJ. Cell adhesion on microstructured fibronectin gradients fabricated by multiphoton excited photochemistry. Cell Mol Bioeng 2012;5:307–19.
[41] Lord MS, Foss M, Besenbacher F. Influence of nanoscale surface topography on protein adsorption and cellular response. Nano Today 2010;5:66–78.
[42] Wei JH, Igarashi T, Okumori N, Maetani T, Liu BL, Yoshinari M. Influence of surface wettability on competitive protein adsorption and initial attachment of osteoblasts. Biomed Mater 2009;4:045002.
[43] Clarke B, Kingshott P, Hou X, Rochev Y, Gorelov A, Carroll W. Effect of nitinol wire surface properties on albumin adsorption. Acta Biomater 2007;3:103–11.
[44] Cai K, Bossert J, Jandt KD. Does the nanometre scale topography of titanium influence protein adsorption and cell proliferation? *Colloid Surface B* 2006;49:136–44.
[45] Sivaraman B, Latour RA. The relationship between platelet adhesion on surfaces and the structure versus the amount of adsorbed fibrinogen. Biomaterials 2010;31:832–9.
[46] Koh LB, Rodriguez I, Venkatraman SS. Conformational behavior of fibrinogen on topographically modified polymer surfaces. Phys Chem Chem Phys 2010;12:10301–8.
[47] Shen JW, Wu T, Wang Q, Pan HH. Molecular simulation of protein adsorption and desorption on hydroxyapatite surfaces. Biomaterials 2008;29:513–32.